

# Role of oxygen-containing groups on MWCNTs in enhanced separation and permeability performance for PVDF hybrid ultrafiltration membranes

Jilan Ma<sup>a</sup>, Yufen Zhao<sup>a</sup>, Zhiwei Xu<sup>a,\*</sup>, Chunying Min<sup>b</sup>, Baoming Zhou<sup>a</sup>, Yinglin Li<sup>a</sup>, Baodong Li<sup>a</sup>, Jiarong Niu<sup>a</sup>

<sup>a</sup> State Key Laboratory of Hollow Fiber Membrane Materials and Processes, School of Textiles, Tianjin Polytechnic University, Tianjin 300387, PR China

<sup>b</sup> School of Material Science and Engineering, Jiangsu University, Zhenjiang 212013, PR China

## HIGHLIGHTS

- PVDF ultrafiltration membranes were prepared with pristine and oxidized MWCNTs.
- Contact angle of membranes decreased from 75.8° to 54.7° (1wt.% oxidized MWCNTs).
- The water flux of membrane increased 11 times by adding 1wt.% oxidized MWCNTs.
- Oxidized MWCNTs outperformed remarkably pristine MWCNTs in membrane performance.

## ARTICLE INFO

### Article history:

Received 15 December 2012

Received in revised form 1 April 2013

Accepted 10 April 2013

Available online 10 May 2013

### Keywords:

Organic–inorganic hybrid membranes

Multi-walled carbon nanotubes

Oxygen-containing groups

Hydrophilicity

Permeability

Rejection

## ABSTRACT

To investigate the effect of the oxygen-containing groups of inorganic modifiers on polyvinylidene fluoride (PVDF) membrane performance, the PVDF/multi-walled carbon nanotube (MWCNT) hybrid ultrafiltration membranes were prepared via phase inversion by dispersing pristine and different dosage oxidized MWCNTs ranging from 0.2 wt.% to 2 wt.% in PVDF casting solutions. An increment in the porosity, pore size and surface roughness of the membranes was observed by the addition of pristine and oxidized MWCNTs. The rejection increased 22.2% in the content of 0.5 wt.% oxidized MWCNTs. The contact angle of membranes decreased from 75.8° (pure PVDF) to 54.7° (PVDF/1 wt.% oxidized MWCNTs), and 11 times increase in water flux was also indicated with the incorporation of 1 wt.% oxidized MWCNTs, which was considered as the optimum dosage. More importantly, the architecture and performance of PVDF/oxidized MWCNTs hybrid membranes outperformed PVDF/pristine MWCNTs hybrid membranes remarkably in the same content (1 wt.%), which can be ascribed to the presence of hydrophilic oxygen-containing groups. This work demonstrated that the oxygen-containing groups of inorganic fillers played a critical role in determining the structures, morphologies and performances of ultrafiltration membranes.

© 2013 The Authors. Published by Elsevier B.V. All rights reserved.

## 1. Introduction

Polymer–inorganic nanocomposite membranes [1–4] which were formed by uniformly dispersing inorganic particles in polymer matrix have received much attention in the field of gas separation, pervaporation and ultrafiltration (UF) for many years. They presented an interesting approach to improve the separation properties of polymer membranes because they possess properties of both organic and inorganic membranes [5–12]. An appropriate porous membrane must have high permeability, good hydrophilicity, and excellent chemical resistance to

the feed streams. In order to obtain high permeability, membranes should have high surface porosity and good pore structure.

Poly(vinylidene fluoride) (PVDF) is a common UF, microfiltration and pervaporation membrane material because of its excellent chemical resistance and thermal stability. However, the hydrophobic nature of PVDF often results in severe membrane fouling and permeability decline, which has become a conspicuous drawback for their application in water treatment. Many research have carried out to improve the membrane performances by adding three-dimensional (3D) inorganic nanoparticles such as Al<sub>2</sub>O<sub>3</sub> [8,13], SiO<sub>2</sub> [7,14], TiO<sub>2</sub> [15], ZrO<sub>2</sub> [9], Fe<sub>3</sub>O<sub>4</sub> [11,12], and LiClO<sub>4</sub> [10,16]. However, the modification of PVDF blending with nanoparticles has been widely explored for improving the hydrophilicity, permeability, rejection, mechanical strength and effective control of membrane surface performance, the nanoparticle-

\* Corresponding author. Tel./fax: +86 22 83955231.

E-mail address: [xuzhiwei@tjpu.edu.cn](mailto:xuzhiwei@tjpu.edu.cn) (Z. Xu).

organic hybrid membrane has some inherent and significant drawbacks. When the nanoparticles with low specific surface area were dispersed to casting solutions, the high concentration could induce nanoparticles to aggregate, resulting in defective pore structure of the membranes and the decline of modification effects [17,18]. Hence, it is very important to redesign nanoparticle structure with high specific surface as an inorganic addition material to lower the additive proportion. Recently, one-dimensional (1D) nanostructures of various morphologies, including nanowires, nanofibers, nanorods and nanotubes, have been introduced to improve the membrane performances [19–21]. But it is difficult for these nanostructures to possess oxygen-containing functional groups on the surface owing to their inherent characteristic, which are expected to improve the hydrophilicity markedly of membranes. As a result, the nanostructures with high specific surface and abundant oxygen-containing functional groups are attractive for the PVDF hybrid membrane.

Carbon nanotubes (CNTs) have attracted a great deal of attention because of their high specific surface area, easy functionalization, chemical stability and thermal conductance [22–25], and have gained more attention as one of these additives recently. CNTs are also one of the candidates to create a surface with a roughness at micro/nanometer level owing to their rigid cylindrical nanostructures with a diameter ranging from about 1 nm to dozens of nanometers and length ranging from hundreds of nanometers to micrometers, which could lead to the increase of efficient filtration area and permeability of the composite membranes [26]. In some literatures, the increments in special parameters like hydrophilicity, permeability and rejection have been studied because of adding CNTs to polymeric membranes [27–31]. However, the role of unique physical and chemical structure of CNTs including high specific surface, one-dimensional architecture and rich oxygen-containing groups in tailoring the performance of hybrid membrane has not been investigated deeply. In this research, the effects of oxygen-containing groups on the membrane morphology and performance were investigated.

Moreover, a series of novel high-performance PVDF ultrafiltration membranes, with pristine and acid oxidation treated multi-walled carbon nanotubes (MWCNTs) as an additive, were successfully fabricated using the phase separation method, respectively. The objective of this work was to systematically reveal the effects of oxidized MWCNTs with high aspect ratio and rich oxygen-containing functional groups on performance of hybrid membranes. The influence of oxidized MWCNT concentrations on the membrane morphology and performance and the comparison between pristine and oxidized MWCNTs were investigated. Then a series of experiments, such as water contact angle (CA), water flux, bovine serum albumin (BSA) rejection, porosity, scanning electron microscopy (SEM) and atomic force microscopy (AFM) measurements, were carried out for membrane characterization.

## 2. Experimental

### 2.1. Materials

PVDF (FR904) was purchased from Shanghai 3F New Materials Co. Ltd., China. N, N-dimethylacetamide (DMAc, >99.5%, reagent) and polyvinylpyrrolidone (PVP) were purchased from Tianjin Weichen Chemical Reagent Co. Ltd., China. Multi-walled carbon nanotubes (MWCNTs, with diameters of 10–50 nm and length of 1–30  $\mu\text{m}$ ) were obtained from Nanjing XF Nanomaterial Science and Technology Co. Ltd., China. The purity of the received MWCNT is 95%. The distilled water was used as the nonsolvent for the polymer precipitation.

### 2.2. Preparation of oxidized MWCNTs

In order to remove the impurities of raw MWCNTs (such as the metallic catalyst particles and amorphous carbon) and introduce hydrophilic functional groups on the surface of MWCNTs, 2 g raw MWCNTs were soaked in 160 mL solution of  $\text{H}_2\text{SO}_4/\text{HNO}_3$  (3/1, v/v) and were

heated to 70 °C for 8 h without stirring [32]. The solution was diluted with 2 L deionized water and filtered through a 0.45  $\mu\text{m}$  membrane. The oxidized MWCNTs were washed with deionized water to reach to neutral pH, and dried at 55 °C in a vacuum for 8 h.

### 2.3. Characterization of MWCNTs

Fourier-transform infrared spectroscopy (FTIR) was used to identify introduced functional groups onto the surface of acid oxidation treated MWCNTs. The surface morphology of MWCNTs was examined using transmission electron microscopy (TEM, Hitachi 7650). The samples were dispersed by sonication in a mixture of ethanol, and then deposited on a holey carbon TEM grid and dried.

### 2.4. Membrane preparation

PVDF/MWCNT hybrid membranes were prepared by the phase inversion method [33]. Casting dopes were prepared by dispersing the MWCNTs in the solvent via an ultrasonicator for at least 2 h and adding PVDF and PVP to the casting dopes under stirring. The weight content of oxidized MWCNTs in the total weight of the membrane-forming materials was 0, 0.2, 0.5, 1 and 2 wt.%, respectively, and these membranes were named as POM-0, POM-0.2, POM-0.5, POM-1, and POM-2, correspondingly. For comparison, the PVDF hybrid membrane with 1 wt.% pristine MWCNTs (named as PPM-1) was prepared by the most suitable proportion for membrane with oxidized MWCNTs. In order to obtain optimal dispersions of the nanomaterials in the polymer solutions, agitation was required for 48 h. After cooling the solution to room temperature, it was ultrasonicated for 30 min to release air bubbles, and then was degassed to ensure complete removal of air bubbles before membrane casting.

In this research, PVP was used to enhance the porosity of PVDF UF membranes [34], and it might increase the hydrophilicity of membrane due to the residue trapped in the membrane matrix [35]. Therefore, to highlight the special contribution of MWCNTs in hydrophilicity and permeability, a hydrophilic pure membrane was fabricated as a control by proper over-dosage of PVP (added 20 wt.% PVP, by weight of PVDF, determined after several tests).

The cast solution was spread into liquid film on a glass plate with a steel knife, and after a 30 s exposure in the air, the plate was immersed in a coagulation bath of distilled water (25 °C). The formed membranes were peeled off and subsequently washed with distilled water to remove residual solvent. Several pieces of membranes of each kind were dried in the air at room temperature for structure and performance measurements. The residual membranes were kept in distilled water for filtration tests.

### 2.5. Characterization of membranes

#### 2.5.1. Morphology observation

The surface and cross-sectional structures of the membranes were examined by SEM (Quanta 200, Holland). Cross-sections were prepared by fracturing the membranes at the temperature of liquid nitrogen. All specimens were coated with a thin layer of gold before being observed using SEM. AFM (CSPM5500) was employed to analyze the surface morphology and roughness of the membranes. In the range of the scan areas 10  $\mu\text{m} \times 10 \mu\text{m}$ , roughness parameters could also be obtained with the AFM analysis software, small squares of the prepared membranes (approximately 1  $\text{cm}^2$ ) were cut and glued on the glass substrate before being scanned (10  $\mu\text{m} \times 10 \mu\text{m}$ ).

#### 2.5.2. UF performances

The permeation flux and rejection of the membranes were measured by UF experimental equipment. The rejection tests were carried out with an aqueous solution of BSA (molecular weight = 67,000) (1  $\text{g} \cdot \text{L}^{-1}$ ). All experiments were conducted at 25 °C and under the

feed pressure of 0.1 MPa. The newly prepared flat-sheet membranes were pre-pressured at 0.1 MPa using the pure water for 1 h before measurement, and then the pure water permeation and rejection for the BSA solution were measured. The concentrations of BSA in the permeation and feed solution were determined by an UV-spectrophotometer (Shimadzu UV-2450, Japan). The permeation flux and rejection were defined as formulae (1) and (2), respectively.

$$F = \frac{Q}{A \times T} \quad (1)$$

$$R = \left(1 - \frac{C_p}{C_f}\right) \times 100\% \quad (2)$$

where  $F$  was the permeation flux of membrane for pure water ( $\text{L} \cdot \text{m}^{-2} \cdot \text{h}^{-1}$ ),  $Q$  was the volume of permeate pure water (L),  $A$  was the effective area of membrane ( $\text{m}^2$ ) and  $T$  was the permeation time (h).  $R$  was the rejection to BSA (%),  $C_p$  and  $C_f$  were the concentrations of BSA in the permeation and feed solution, respectively.

### 2.5.3. Porosity and mean pore size calculation

The membrane porosity  $P_r$  (%) was defined as the volume of the pores divided by the total volume of the porous membrane. It could usually be determined by gravimetric method, determining the weight of liquid (here pure water) contained in the membrane pores [36].

$$P_r = \frac{(w_1 - w_2)/d_w}{(w_1 - w_2)/d_w + w_2/d_p} \times 100\% \quad (3)$$

where  $w_1$  was the weight of the wet membrane (g),  $w_2$  was the weight of the dry membrane (g),  $d_w$  was the pure water density ( $0.998 \text{ g} \cdot \text{cm}^{-3}$ ) and  $d_p$  was the polymer density (as the inorganic content in the membrane matrix was small and  $d_p$  was approximate to  $d_{\text{PVDF}}$ , namely  $1.765 \text{ g} \cdot \text{cm}^{-3}$ ).

The mean pore size [ $r$  (m)] was defined as follows [37]:

$$r = [8 \times (2.9 - 1.75P_r) \cdot \eta L F / 3600 P_r \Delta P]^{1/2} \quad (4)$$

where  $\eta$  is the viscosity of water ( $8.9 \times 10^{-4} \text{ Pa s}$ ),  $L$  is the membrane thickness (m),  $F$  is the pure water flux ( $\text{m}^3/\text{m}^2 \cdot \text{h}$ ), and  $\Delta P$  is the working pressure (Pa).

### 2.5.4. Water CA measurements

The CA between water and the membrane surface was measured with a contact-angle measurement apparatus (JYSP-180 Contact Angle Analyzer) according to the sessile-drop method. Briefly, a water droplet was deposited on a flat homogeneous membrane surface and the contact angle of the droplet with the surface was measured. The value was observed until there was no change in CA during the short measurement period. Each CA was measured five times at five different points of each membrane sample and an average value was calculated.

### 2.5.5. Tensile break strength measurements

The tensile strength and elongation-at-break of the membranes were determined at room temperature using a material tester (YG028, Wenzhou Fangyuan Instrument Co. Ltd. China), and the tensile rate was 10 mm/min. For each specimen, five runs were performed and then averaged.

## 3. Results and discussion

### 3.1. Characterization of MWCNTs

TEM was able to provide the morphology and tubular structure of MWCNTs, including the dispersion of MWCNTs. Fig. 1(a, b) presented TEM images of pristine and oxidized MWCNTs, respectively. MWCNTs were held together as bundles and had very low solubility in most solvents because of their intrinsic van der Waals forces [38]. It was known that acid oxidation treatment shortened nanotubes with carboxyl acid groups mainly on the end tips [39,40]. The length of oxidized MWCNTs was shortened in the range of  $0.2 \mu\text{m}$ – $1.0 \mu\text{m}$  through treatment with a strong acid mixture. Fig. 1a showed some aggregation of original MWCNTs, and Fig. 1b demonstrated that MWCNTs dispersed better due to the increasing of hydrophilic oxygen-containing groups. And acid oxidation treated MWCNTs (Fig. 1b) showed a decrease in the number of longer nanotubes and an increase in the number of shorter nanotubes than that of pristine MWCNTs (Fig. 1a).

Fig. 2 depicted the FTIR absorption spectra of pristine and acid oxidation treated MWCNTs. The peaks emerging at 1400, 1620 and 1700, and 3100–3600  $\text{cm}^{-1}$  were corresponded to C=O, COOH and O–H bonds onto the surface of oxidized MWCNTs, and the results were in good agreement with the results of previous reports [41,42]. Therefore, it was expected that the oxygen-containing surface functional groups introduced in the oxidative cutting process on the MWCNTs

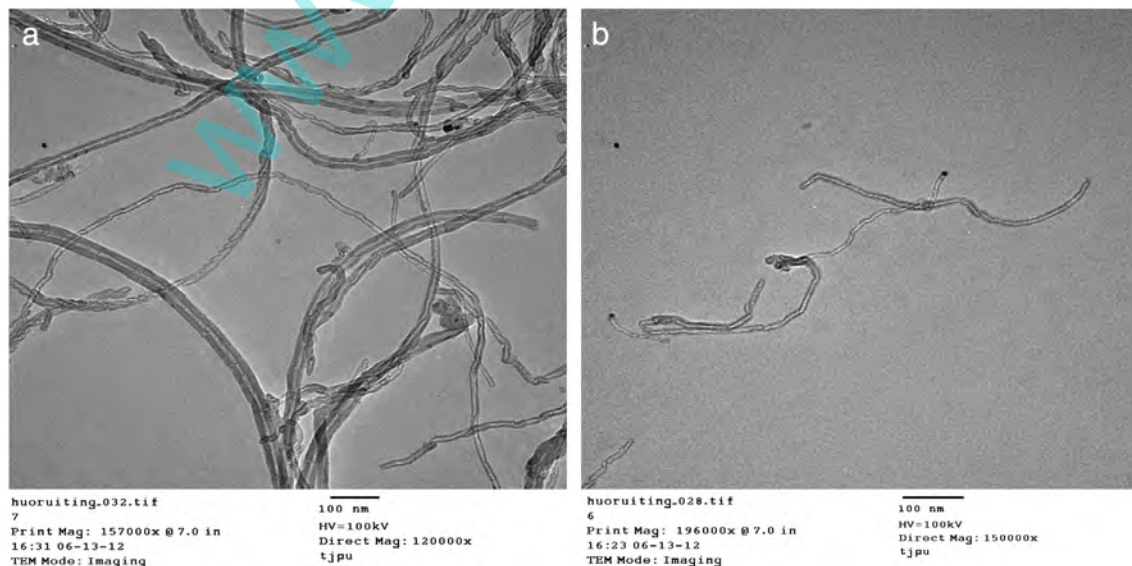


Fig. 1. TEM images of (a) pristine MWCNTs and (b) oxidized MWCNTs.

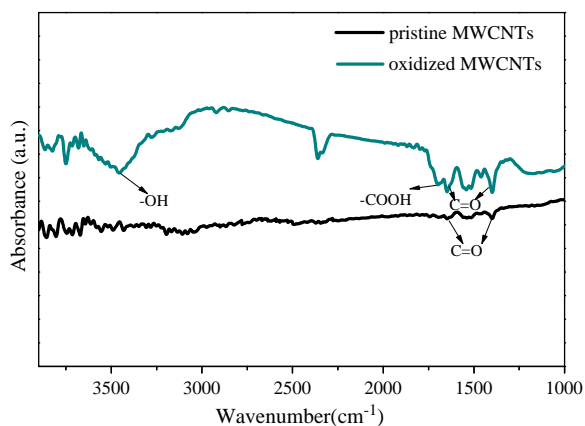


Fig. 2. FTIR spectra of pristine and oxidized MWCNTs.

can greatly enhance the hydrophilicity and permeability of PVDF hybrid membranes. Meanwhile, the hydrophilicity of these functional groups would improve the dispersivity of oxidized MWCNTs in aqueous solution.

### 3.2. Microstructures of membranes

The surface and cross-section morphologies of the PVDF blend membranes were shown in Figs. 3 and 4, respectively. Obviously, there was an evident improvement in surface porosity which could be viewed intuitively from the SEM images (Fig. 3). The larger pores emerged on the surface of the hybrid membranes compared with pure PVDF membrane, which may have a relation to increase of membrane flux. The MWCNTs on the surface of blend membranes were observed when the surface photographs of prepared membranes were compared as presented in Fig. 3 (labelled as red circle). The

membranes prepared by PVDF/0.5 wt.% oxidized MWCNTs and PVDF/1 wt.% oxidized MWCNTs demonstrated the strong change in pore size and morphology. However, when the content of oxidized MWCNTs was increased further, especially over 1 wt.%, the pore size started to decrease, and it was easy to form a relatively dense structure. This was probably due to the increased viscosity which delayed phase separation by the added high-proportion hydrophilic MWCNTs. In addition, the similar amelioration could also be noted for PPM-1 hybrid membrane compared with POM-0 membrane, but not as palpable as that of oxidized PVDF/MWCNT hybrid membranes. The surface pore size and density of PPM-1 membrane were similar to those of the hybrid PVDF membranes with low content of oxidized MWCNTs, which have small change compared with pure PVDF membrane (shown in Fig. 3).

The cross-sections of all the membranes presented the same asymmetric and highly inhomogeneous structure with a selective thin microporous surface skin on large voids and finger-like cavities. This structure was mainly due to the high mutual diffusivity of water and DMAc [43]. As could be seen in Fig. 4, comparing the upper side of the finger-like cavities, there were many larger fingerlike pores in the hybrid membrane. The size of the macro-voids was observed to increase with the content of MWCNTs, and the water molecule could pass through the membrane easier, which may be another reason for the increase of membrane water flux. This result may be explained by the fast exchange of solvent and non-solvent in the phase inversion process due to the hydrophilic MWCNTs [44], and occurring interactions between components in the casting solution and phase inversion kinetics.

Roughness would also influence the performance of hybrid membrane, and the parameters could be obtained with the AFM analysis software. There exists mean roughness ( $R_a$ ), which is the mean value of surface area relative to the center plane, for which the volume enclosed by the image above and below this plane is equal.

Fig. 5 displayed three-dimensional AFM images of the membrane external surfaces. According to the AFM images, obviously the surface of hybrid membranes was rather rougher than pure PVDF membrane.

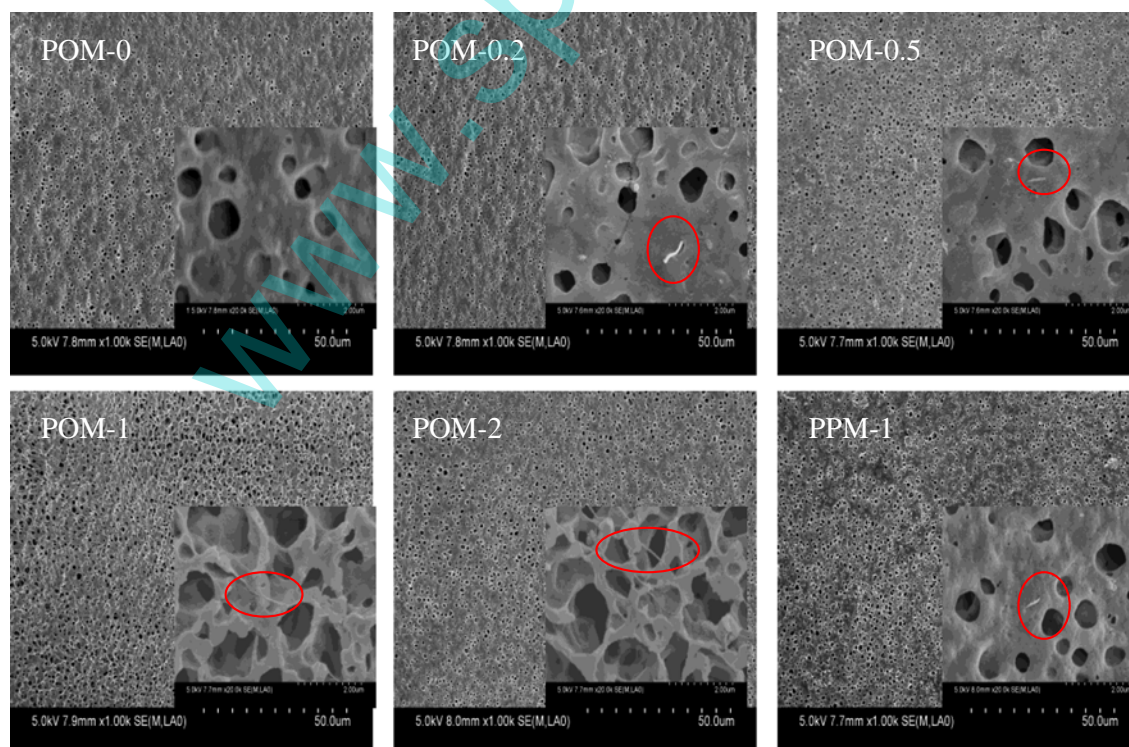


Fig. 3. The surface views of membranes with different blend compositions. (For interpretation of the references to color in this figure, the reader is referred to the web version of this article.)



Fig. 4. The cross-section views of membranes with different blend compositions.

The roughness parameters of the surfaces of the membranes existed mean roughness (Ra), root mean square (Rq), and mean difference in the height between the five highest peaks and the five lowest valleys (Rz). The surface roughness parameters (Ra) of the membranes

were calculated by AFM software in  $10\ \mu\text{m} \times 10\ \mu\text{m}$  scan size and presented in Table 1. This table confirmed that the roughness of the membrane surface initially increased with addition of oxidized MWCNTs up to 1 wt.% and then decreased with further increase of

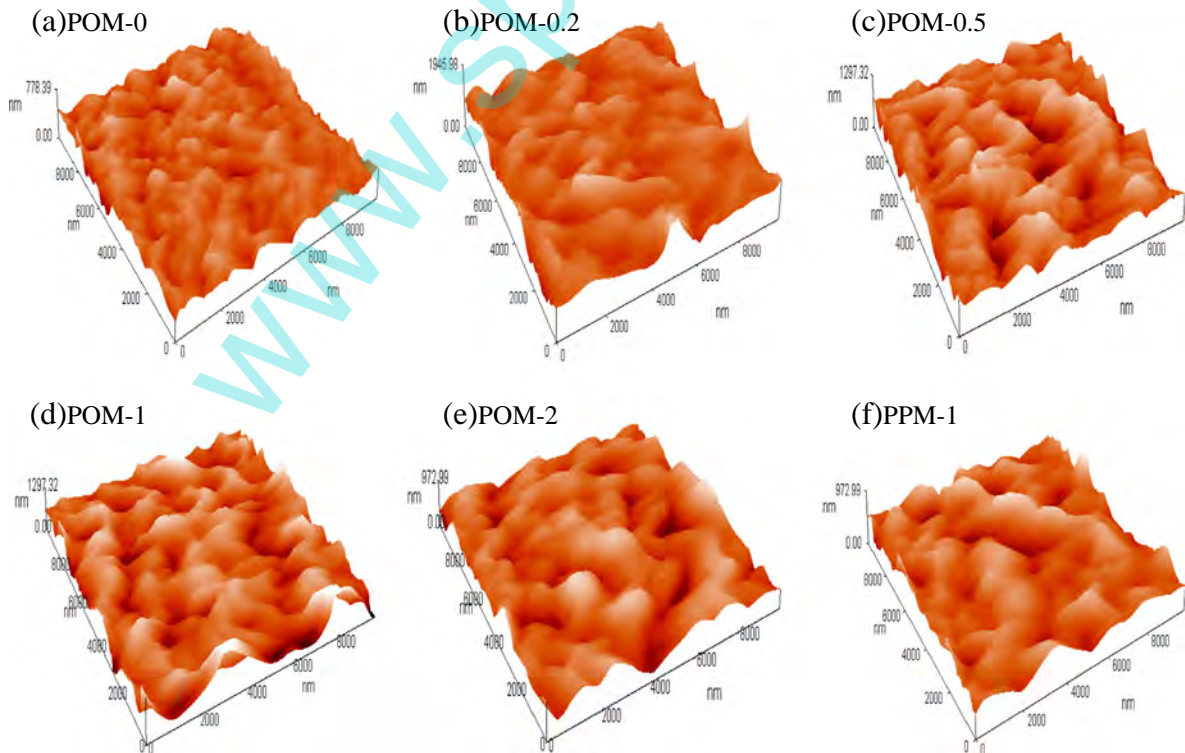


Fig. 5. Surface AFM images of the PVDF hybrid membranes with different concentrations of carbon nanotube. (a) 0%, (b) 0.2%, (c) 0.5%, (d) 1%, (e) 2% oxidized MWCNTs and (f) 1% pristine MWCNTs.

**Table 1**  
Surface parameters of PVDF hybrid membranes.

Membrane	Surface area ( $\mu\text{m}^2$ )	Roughness		
		$R_a$ (nm)	$R_q$ (nm)	$R_z$ (nm)
POM-0	110.3	50.1	64	576
POM-0.2	128.8	120	154	1550
POM-0.5	129.5	134	171	1110
POM-1	140.0	153	194	1290
POM-2	111.5	97	123	835
PPM-1	110.4	90.3	116	836

oxidized MWCNT content. The PVDF membrane with 1 wt.% oxidized MWCNTs had the highest surface roughness value of 153 nm and increased 200% compared with POM-0 membrane. As mentioned, the effect of hydrophilicity of oxidized MWCNTs accelerated the exchange rate between solvent and non-solvent during the phase inversion, when the membrane contained 1 wt.% or less than 1 wt.% oxidized MWCNTs [45,46]. The corresponding membrane had larger pore size (Fig. 3) and rougher surface which will facilitate permeation efficiency and hydrophilicity. However, the roughness of PPM-1 membrane merely increased from 50.1 nm to 90.3 nm but was inferior to that of POM-1. The pristine MWCNTs with less oxygen-containing functional groups on the surface versus oxidized MWCNTs had weaker effects for this exchange rate between solvent and on-solvent during the membrane formation. At 2 wt.% concentration of oxidized MWCNTs, the viscosity of the casting solution increased strongly. The high viscosity for casting solution hindered the exchange between solvent and non-solvent, leading to formation of a membrane with smooth surface with smaller pore size and denser structure.

### 3.3. Porosity and mean pore size of membranes

The effects of the oxidized and pristine MWCNTs on the porosity and mean pore size were shown in Fig. 6. Both porosity and mean pore size of membranes were increased with the addition of oxidized MWCNTs. The porosity of prepared membranes ranged from 82% to 86%. When the content of oxidized MWCNTs was 1 wt.%, the porosity reached its peak value of 86% and increased by 5% compared with the pure PVDF membranes. However, when the concentrations of oxidized MWCNTs were increased further (2 wt.%), a denser structure in sub-layer with the fewer finger-like pore was formed. This was probably due to the strong increase in the viscosity of casting solution with the excess addition of oxidized MWCNTs. The similar variation trend was also exhibited in the data of the mean pore size with different content of oxidized MWCNTs. When the content of oxidized MWCNTs was 1 wt.%, the mean pore size reached its peak value of

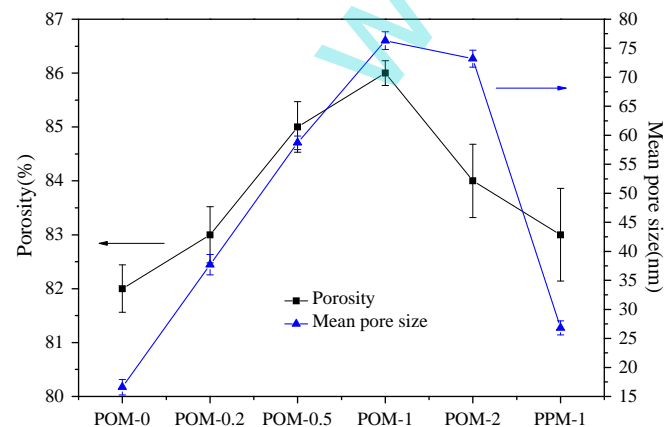


**Fig. 6.** Effects of the MWCNTs on the porosity and mean pore size of the hybrid membranes.

76.3 nm and increased by 360% compared with POM-0 membrane. However, the porosity and mean pore size improvement of PPM-1 membrane were not obvious. The difference could be interpreted as follows. Oxidized MWCNTs were a kind of hydrophilic material. During the membrane preparation process, the diffusion rate between gels (water) and solvent (DMAc) could be accelerated by oxidized MWCNTs. The occurrence of phase separation process, which was good for the generation of polymer-poor phase, was also facilitated by the presence of oxidized MWCNTs in membrane preparation process. In contrast, pristine MWCNTs contained less hydrophilic groups, which might not accelerate the diffusion rate between water and DMAc in membrane. Thus, the existence of oxidized MWCNTs could be more beneficial to the formation of membranes with high porosity and mean pore size than those of pristine MWCNTs.

### 3.4. Hydrophilicity of the membranes

The CA results were shown in Fig. 7, from which an obvious trend could be drawn that the CA values gradually decreased when the amount of oxidized MWCNTs was increased, suggesting the increase of hydrophilicity of PVDF membrane surface. The CA value of POM-1 even achieved  $54.7^\circ$  and decreased  $21.1^\circ$  than that of POM-0. As could be seen in Fig. 7, increasing the oxidized MWCNT amount to more than 1 wt.% did not result in notable enhancement of the hydrophilicity and the CA value of POM-2 was  $53.2^\circ$ . This might be explained by the irregular positioning of MWCNTs in the membrane structure at 2 wt.% oxidized MWCNT content [47], which lead to aggregation and reducing effective surface of nanotubes. In contrast with the control membrane (POM-0), which was deliberately (Section 2.4.) fabricated to be hydrophilic (CA  $75.8^\circ$ ), the hybrid membranes obtained a further decrease of CA, suggesting the positive effect of oxidized MWCNTs on membrane surface hydrophilicity. As a result, this might play a favorable role in elevating the pure water flux of the hybrid membranes. Meanwhile, the hydrophilicity improvement of PPM-1 was less than that of POM-1. This was due to the hydrophilic groups on the membrane structure which forms by addition of oxidized MWCNTs in the PVDF casting solution.

### 3.5. Pure water flux and rejection ratio of membranes

The data of the pure water flux of different membranes were depicted in Fig. 8(a). When the content of oxidized MWCNTs ranged from 0 to 2 wt.%, the pure water flux went up with increasing of oxidized MWCNT contents in the casting solution. In the current experiment, a transmembrane pressure of 0.1 MPa was employed. Under this pressure differential, the water flux of the POM-1 membrane reached a peak value of  $1225 \text{ L}/(\text{m}^2 \text{ h})$  and increased approximately 11

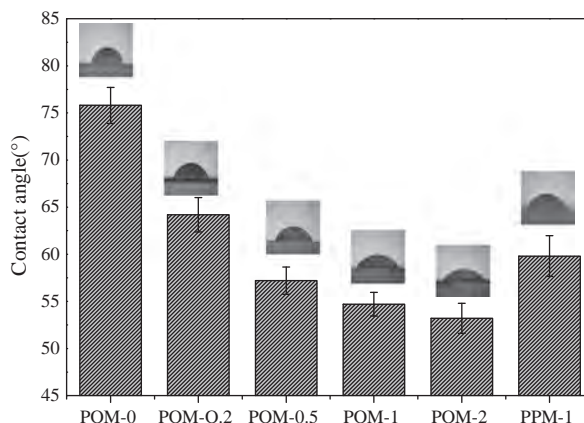


**Fig. 7.** Results of the CA measurements for the hybrid membranes.

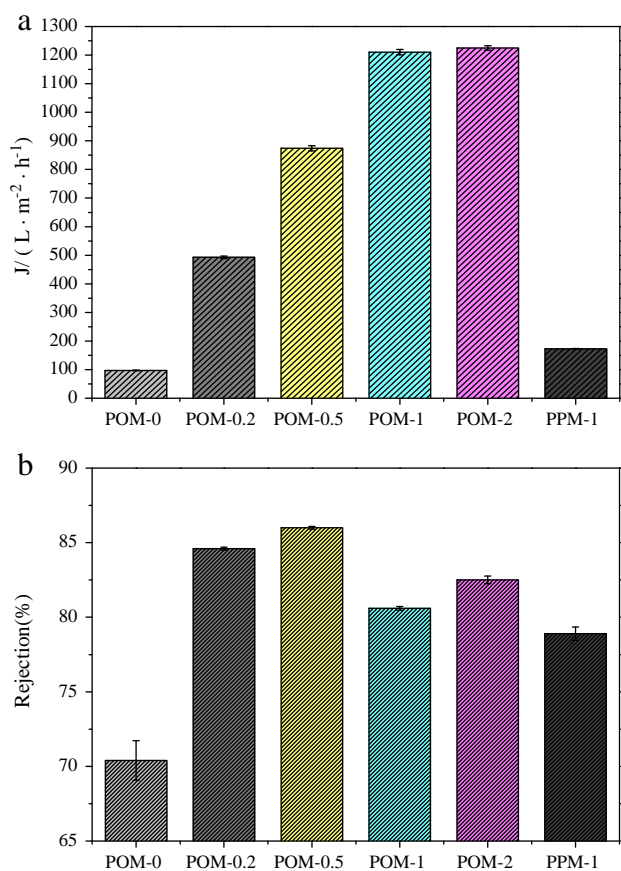


Fig. 8. Effects of the MWCNTs on (a) pure water flux and (b) rejection ratio of the hybrid membranes.

times compared with the pure membrane. Further addition of oxidized MWCNTs in the casting solution resulted in the invisible change for the pure water flux of membrane. Considering the results in Fig. 8a, the improvement of POM-(0.2–2) permeability might be due to various factors. Firstly, the hybrid membranes were all endowed with advantageous porous surface and favorable inner structure, which undoubtedly played a positive role in promoting membrane permeability [48]. Secondly, the addition of oxidized MWCNTs resulted in the increase of membrane hydrophilicity (Fig. 7), which might also act favorably in promoting the water permeability. However, because there were less oxygen-containing functional groups of pristine MWCNTs, which consequently lead to the limited improvement in porosity, mean pore size and hydrophilicity of membranes. Consequentially, PVDF/oxidized MWCNT membranes with high porosity and hydrophilicity showed good water permeability compared with PVDF/pristine MWCNT membranes.

The BSA rejection ratio results of different membranes were also depicted in Fig. 8b. Generally, CNTs have exhibited the capability for the removal of albumin as a type of adsorbent [49]. As could be seen in Fig. 8b, the BSA rejection increased significantly when the MWCNT content was increased to 0.5 wt.%. And the data showed that POM-0.5 membrane had the highest BSA rejection (86.0%), which increased 22.2% compared with that of the pure PVDF membranes. However, when the content of oxidized MWCNTs was increased further, especially at 1 wt.% of oxidized MWCNTs, the membrane surface porosity and pore size were strongly increased, resulting in the decrease of BSA rejection. However, when the concentrations of oxidized MWCNTs increased to 2 wt.%, the high density of MWCNTs in the casting solution led to an increase in the viscosity of solution. This will

prevent the phase exchange between the solvent and non-solvent during the phase separation process and slow down the precipitation of the membrane, consequently, a relative smaller porous membrane was formed. Thus, the rejection increased again. Moreover, the decline in hydrophobic interaction between BSA protein and hydrophilic surface of membrane might be a reason for slight increase in BSA rejection. Thereby, the oxidized MWCNTs endowed higher rejection for hybrid membranes than pristine MWCNTs.

### 3.6. Mechanical strength of membranes

Mechanical properties of membranes were determined by the data on tensile strength and elongation-at-break of membranes. Table 2 showed the tensile properties of the PVDF hybrid membranes. Compared to the pure PVDF membrane, the tensile strength of PVDF/oxidized MWCNT membranes was firstly increased with the addition of oxidized MWCNTs when the oxidized MWCNT concentration was 0.2 wt.%, and afterwards declined from 0.87 MPa to 0.66 MPa as the oxidized MWCNT concentration was further increased [50]. However, the elongation-at-break of hybrid membranes decreased markedly with increased of the oxidized MWCNT content. The decrease in performance especially for the PVDF membranes with microporous surface was not surprising taking into account the results of the finger-like cavities appeared larger and sparser characterizations (shown in Fig. 4) and the weak interface compatibility between hydrophilic oxidized MWCNTs and hydrophobic PVDF matrix. This also may be due to the fact that the large MWCNT aggregates appeared with the increase of MWCNT content, which would accelerate the fracture process of membranes. The tensile strength of PPM-1 membrane merely decreased from 0.84 MPa to 0.71 MPa, and the elongation-at-break of PPM-1 membrane decreased from 14.71% to 4.81%, thus they were inferior to those of POM-1. This indicated that MWCNTs had a negative effect on PVDF mechanical properties. The trend was explained by the fact that there was no strong affinity between PVDF and untreated MWCNTs due to the low-surface energy of PVDF. As a result, the compatibility between MWCNTs and PVDF matrix needs further investigation to obtain excellent performance of blend membranes by surface functionalization (such as fluorination) of CNTs.

### 3.7. Discussion

An increment in the porosity, pore size and surface roughness of the membranes was observed by increasing oxidized MWCNT content up to 1 wt.%. Further addition of oxidized MWCNTs caused a reduction in porosity and roughness of formed membrane, but at 2 wt.% loading they were still higher compared with those of pure PVDF membranes. Certain amount of oxygen-containing functional groups on the oxidized MWCNTs was beneficial to the membrane hydrophilicity. The hydrophilic MWCNTs on the surface of hybrid membranes were observed as presented in Fig. 3, which have a relation to increase of membrane hydrophilicity. It was well known that water permeation flux was strongly determined by the surface roughness, hydrophilicity, porosity and pore size of membranes [48]. Consequently the increased membrane hydrophilicity played a favorable role in elevating the pure

Table 2  
Mechanical properties of PVDF hybrid membranes.

Membrane	Tensile strength (MPa)	Elongation-at-break (%)
POM-0	0.84 ± 0.18	14.71 ± 2.37
POM-0.2	0.87 ± 0.09	8.93 ± 1.52
POM-0.5	0.84 ± 0.11	8.49 ± 1.16
POM-1	0.78 ± 0.05	7.48 ± 1.04
POM-2	0.66 ± 0.10	6.75 ± 1.33
PPM-1	0.71 ± 0.08	4.18 ± 0.41

**Table 3**  
Comparative results of modified PVDF membranes with different inorganic fillers.

Inorganic fillers	Inorganic fillers dimensionality	Optimum dosage of inorganic material (PVDF, g/g)	Decreased contact angle (°)	Rate of change in water flux (%)	Rate of change in rejection (%)	Rate of change in tensile strength (%)	Rate of change in elongation-at-break (%)	Reference
ZnO	3D	6.7%	~13	↑~75	–	↑~7.8	↓~18.8	[6]
SiO <sub>2</sub>	3D	5%	–	↑~140	–	↑~109	↑~83	[7]
	3D	3%	29.5	↑~275	↓~8	–	–	[14]
Al <sub>2</sub> O <sub>3</sub>	3D	2%	26.2	↑~400	↑1	↑~50	↑~55	[8]
ZrO <sub>2</sub>	3D	150%	–	↑~500	–	–	–	[9]
Fe <sub>3</sub> O <sub>4</sub>	3D	70%	–	↑~270	↑~18	↑~8.6	–	[12]
TiO <sub>2</sub>	3D	2%	4	↑~19	↓~3	–	–	[16]
	1D	5%	48.3	↑~66	↑~7	↑~33	↑~59	[20]
Pristine MWCNTs	1D	1%	16	↑~78	↑~12	↓~15	↓~71	In this research
Oxidized MWCNTs	1D	1%	21.1	↑~1100	↑~15	↓~7.1	↓~49	In this research

↑ increased, ↓ decreased, – no research.

water flux. The enlarged roughness could lead to an increase of efficient filtration area in the hybrid membranes, successively resulting in an increase of the membrane water flux. These results showed that increased membrane surface roughness did not have a negative effect on membrane performance; rather, it effectively improved the permeating flux. In addition, the BSA rejection of hybrid membranes was increased significantly because of the well albumin adsorption of MWCNTs (Fig. 8b). Within the dosage range in this study, the optimum oxidized MWCNT dosage was found ideal lying around 1% of membrane weight.

The morphology and performance of PVDF/pristine MWCNT membrane surpassed those of the pure PVDF membrane but far less than those of oxidized MWCNT/PVDF membranes, which attributed to the less oxygen-containing functional groups on the surface of pristine MWCNTs (shown in Fig. 2).

Comparing with the proportion of inorganic fillers in previous literature (Table 3), the content of pristine and oxidized MWCNTs with high specific surface area in hybrid membranes was much lower. However, our hybrid membranes put up a good performance. As could be seen in Fig. 8 and Table 3, the PVDF/oxidized MWCNT hybrid membranes exhibited higher permeability and rejection than those including pristine MWCNTs and other inorganic nanomaterials, although they contained the much low proportion of additive. Moreover, there was a notable improvement in hydrophilicity of PVDF/oxidized MWCNT membrane with low concentration of oxidized MWCNTs. These results were owing to the limited performance improvement for membrane, which was significantly affected by the absence of oxygen-containing functional groups on pristine MWCNTs and other nanomaterials. However, due to the hydrophilicity of oxidized MWCNTs resulting in a larger and sparser porous structure, the mechanical strength of PVDF/oxidized MWCNT membranes had a little decline compared with the membranes containing other inorganic fillers. As a result, it can be concluded that oxidized MWCNTs open up a new opportunity to improve the performance of ultrafiltration membranes.

#### 4. Conclusions

PVDF ultrafiltration membranes were synthesized using the phase inversion process, and the effect of oxidized and pristine MWCNTs on performance of PVDF hybrid membranes has been investigated. The investigation results have been enumerated.

- (1) The PVDF/oxidized MWCNT hybrid membranes had higher porosity, mean pore size and roughness on their surface than pure PVDF membrane. The hydrophilicity of the hybrid membrane was enhanced as oxidized MWCNT content increased and the water contact angle decreased from 75.8° (POM-0) to 54.7° (POM-1). Accordingly, the enhancement was indicated by 11 times increase in water flux and 22.2% increase in BSA rejection when the membranes were blended by 1 wt.% oxidized MWCNTs. As such, within the dosage range in this study, the

addition of 1 wt.% oxidized MWCNTs was recommended for PVDF membrane modification. However, the mechanical performance for hybrid membranes was slightly reduced.

- (2) Comparative studies indicated that the architecture and performance of PVDF/oxidized MWCNT hybrid membranes outperform remarkably those of PVDF/pristine MWCNT hybrid membranes in the same content (1 wt.%), which can be ascribed to the presence of hydrophilic oxygen-containing groups such as –OH, –COOH etc.

The oxygen-containing functional groups on surface of inorganic nanomaterials played a crucial role in the separation and permeability improvement of polymer–inorganic hybrid membranes. In view of the excellent performance of PVDF/MWCNT hybrid membranes, in combination with unique nature of MWCNTs such as the high specific surface and easy functionalization, the functionalized MWCNTs might become a promising modifier for ultrafiltration membranes in future applications.

#### Nomenclature

UF	ultrafiltration
PVDF	polyvinylidene fluoride
3D	three-dimensional
1D	one-dimensional
CNTs	carbon nanotubes
MWCNTs	multi-walled carbon nanotubes
CA	contact angle
BSA	bovine serum albumin
SEM	scanning electron microscopy
AFM	atomic force microscopy
DMAC	dimethylacetamide
PVP	polyvinylpyrrolidone
FTIR	Fourier transform infrared spectroscopy
TEM	transmission electron microscopy
Ra	mean surface roughness (nm)
F	pure waterflux (L·m <sup>-2</sup> ·h <sup>-1</sup> )
Q	the volume of permeate pure water (L)
T	the permeation time (h)
A	the effective area of membrane (m <sup>2</sup> )
R	the rejection rate to BSA (%)
C <sub>F</sub>	concentration of feed (mg/L)
C <sub>P</sub>	concentration of permeate (mg/L)
P <sub>r</sub>	membrane porosity (%)
w <sub>1</sub>	the weight of wet membrane (g)
w <sub>2</sub>	the weight of dry membrane (g)
d <sub>w</sub>	the pure water density (g·cm <sup>-3</sup> )
d <sub>p</sub>	the polymer density (g·cm <sup>-3</sup> )
r	mean pore size
η	viscosity of water (Pa s)
L	membrane thickness (m)
ΔP	working pressure (Pa)

## Acknowledgments

The work was funded by the National Natural Science Foundation of China (11175130), the Natural Science Foundation of Tianjin, China (10JCYBJC02300), the China Postdoctoral Science Foundation (2012M520578, 20100481092) and the Jiangsu Planned Projects for Postdoctoral Research Funds (1202067C, 1002031C).

## References

- [1] M.L. Sforca, I.V.P. Yoshida, S.P. Nunes, Organic–inorganic membranes prepared from polyether diamine and epoxy silane, *J. Membr. Sci.* 159 (1999) 197–207.
- [2] A. Bottino, G. Capannelli, V. D'Asti, P. Piaggio, Preparation and properties of novel organic–inorganic porous membranes, *Sep. Purif. Technol.* 22–23 (2001) 269–275.
- [3] C. Cornelius, C. Hibshman, E. Marand, Hybrid organic–inorganic membranes, *Sep. Purif. Technol.* 25 (2001) 181–193.
- [4] X.J. Liu, Y.L. Peng, S.L. Ji, A new method to prepare organic–inorganic hybrid membranes, *Desalination* 221 (2008) 376–382.
- [5] H.L. Cong, M. Radosz, B.F. Towler, Y.Q. Shen, Polymer–inorganic nanocomposite membranes for gas separation, *Sep. Purif. Technol.* 55 (2007) 281–291.
- [6] S. Liang, K. Xiao, Y.H. Mo, X. Huang, A novel ZnO nanoparticle blended polyvinylidene fluoride membrane for anti-irreversible fouling, *J. Membr. Sci.* 394 (2012) 184–192.
- [7] A.H. Cui, Z. Liu, C.F. Xiao, Y.F. Zhang, Effect of micro-sized SiO<sub>2</sub>-particle on the performance of PVDF blend membranes via TIPS, *J. Membr. Sci.* 360 (2010) 259–264.
- [8] L. Yan, Y.S. Li, C.B. Xiang, S. Xianda, Effect of nano-sized Al<sub>2</sub>O<sub>3</sub>-particle addition on PVDF ultrafiltration membrane performance, *J. Membr. Sci.* 276 (2006) 162–167.
- [9] A. Bottino, G. Capannelli, A. Comite, Preparation and characterization of novel porous PVDF–ZrO<sub>2</sub> composite membranes, *Desalination* 146 (2002) 35–40.
- [10] M.L. Yeow, Y.T. Liu, K. Li, Preparation of porous PVDF hollow fibre membrane via a phase inversion method using lithium perchlorate (LiClO<sub>4</sub>) as an additive, *J. Membr. Sci.* 258 (2005) 16–22.
- [11] J. Du, L. Wu, C.Y. Tao, C.X. Sun, Preparation and characterization of Fe<sub>3</sub>O<sub>4</sub>/PVDF magnetic composite membrane, *Acta Phys. Chim. Sin.* 20 (2004) 598–601.
- [12] Z.Q. Huang, F. Zheng, Z. Zhang, H.T. Xu, K.M. Zhou, The performance of the PVDF–Fe<sub>3</sub>O<sub>4</sub> ultrafiltration membrane and the effect of a parallel magnetic field used during the membrane formation, *Desalination* 292 (2012) 64–72.
- [13] F. Liu, M.R.M. Abed, K. Li, Preparation and characterization of poly(vinylidene fluoride) (PVDF) based ultrafiltration membranes using nano gamma-Al<sub>2</sub>O<sub>3</sub>, *J. Membr. Sci.* 366 (2011) 97–103.
- [14] S.L. Yu, X.T. Zuo, R.L. Bao, X. Xu, J. Wang, J. Xu, Effect of SiO<sub>2</sub>(2) nanoparticle addition on the characteristics of a new organic–inorganic hybrid membrane, *Polymer* 50 (2009) 553–559.
- [15] F.M. Shi, Y.X. Ma, J. Ma, P.P. Wang, W.X. Sun, Preparation and characterization of PVDF/TiO<sub>2</sub> hybrid membranes with different dosage of nano-TiO<sub>2</sub>, *J. Membr. Sci.* 389 (2012) 522–531.
- [16] D.J. Lin, C.L. Chang, F.M. Huang, L.P. Cheng, Effect of salt additive on the formation of microporous poly(vinylidene fluoride) membranes by phase inversion from LiClO<sub>4</sub>/water/DMF/PVDF system, *Polymer* 44 (2003) 413–422.
- [17] Y.N. Yang, P. Wang, Preparation and characterizations of a new PS/TiO<sub>2</sub> hybrid membranes by sol–gel process, *Polymer* 47 (2006) 2683–2688.
- [18] G.P. Wu, S.Y. Gan, L.Z. Cui, Y. Xu, Preparation and characterization of PES/TiO<sub>2</sub> composite membranes, *Appl. Surf. Sci.* 254 (2008) 7080–7086.
- [19] Y. Wei, H.Q. Chu, B.Z. Dong, X. Li, S.J. Xia, Z.M. Qiang, Effect of TiO<sub>2</sub> nanowire addition on PVDF ultrafiltration membrane performance, *Desalination* 272 (2011) 90–97.
- [20] M. Botes, T.E. Cloete, The potential of nanofibers and nanobiocides in water purification, *Crit. Rev. Microbiol.* 36 (2010) 68–81.
- [21] J.Y. Zhang, Y.T. Zhang, Y.F. Chen, L. Du, B. Zhang, H.Q. Zhang, J.D. Liu, K.J. Wang, Preparation and characterization of novel polyethersulfone hybrid ultrafiltration membranes bending with modified halloysite nanotubes loaded with silver nanoparticles, *Ind. Eng. Chem. Res.* 51 (2012) 3081–3090.
- [22] P.M. Ajayan, Nanotubes from carbon, *Chem. Rev.* 99 (1999) 1787–1799.
- [23] S. Iijima, Helical microtubules of graphitic carbon, *Nature* 354 (1991) 56–58.
- [24] M.S. Dresselhaus, G. Dresselhaus, R. Saito, Physics of carbon nanotubes, *Carbon* 33 (1995) 883–891.
- [25] J.W. Che, T. Cagin, W.A. Goddard, Thermal conductivity of carbon nanotubes, *Nanotechnology* 11 (2000) 65–69.
- [26] T.F. Wu, Y.Z. Pan, L. Li, Fabrication of superhydrophobic hybrids from multiwalled carbon nanotubes and poly(vinylidene fluoride), *Colloids Surf. A: Physicochem. Eng. Aspect* 384 (2011) 47–52.
- [27] E. Celik, L. Liu, H. Choi, Protein fouling behavior of carbon nanotube/polyethersulfone composite membranes during water filtration, *Water Res.* 45 (2011) 5287–5294.
- [28] E. Celik, H. Park, H. Choi, Carbon nanotube blended polyethersulfone membranes for fouling control in water treatment, *Water Res.* 45 (2011) 274–282.
- [29] S. Majeed, D. Fierro, K. Buhr, J. Wind, B. Du, A. Boschetti-De-Fierro, V. Abetz, Multi-walled carbon nanotubes (MWCNTs) mixed polyacrylonitrile (PAN) ultrafiltration membranes, *J. Membr. Sci.* 403 (2012) 101–109.
- [30] H.Q. Wu, B.B. Tang, P.Y. Wu, Novel ultrafiltration membranes prepared from a multi-walled carbon nanotubes/polymer composite, *J. Membr. Sci.* 362 (2010) 374–383.
- [31] J.-H. Choi, J. Jegal, W.-N. Kim, Fabrication and characterization of multi-walled carbon nanotubes/polymer blend membranes, *J. Membr. Sci.* 284 (2006) 406–415.
- [32] K.A. Wepasnick, B.A. Smith, K.E. Schrote, H.K. Wilson, S.R. Diegelmann, D.H. Fairbrother, Surface and structural characterization of multi-walled carbon nanotubes following different oxidative treatments, *Carbon* 49 (2011) 24–36.
- [33] P.P. Wang, J. Ma, Z.H. Wang, F.M. Shi, Q.L. Liu, Enhanced separation performance of PVDF/PVP-g-MMT nanocomposite ultrafiltration membrane based on the NVP-grafted polymerization modification of montmorillonite (MMT), *Langmuir* 28 (2012) 4776–4786.
- [34] K.C. Khulbe, C. Feng, T. Matsuura, The art of surface modification of synthetic polymeric membranes, *J. Appl. Polym. Sci.* 115 (2010) 855–895.
- [35] N. Bolong, A.F. Ismail, M.R. Salim, Effect of polyvinylpyrrolidone (PVP) in binary solution on the performance of polyethersulfone hollow fibre membrane for sodium chloride separation, *International Conference on Advancement of Materials and Nanotechnology 2007, 2010*, pp. 358–362.
- [36] J.F. Li, Z.L. Xu, H. Yang, Microporous polyethersulfone membranes prepared under the combined precipitation conditions with non-solvent additives, *Polym. Adv. Technol.* 19 (2008) 251–257.
- [37] L.P. Zhang, G.W. Chen, H.W. Tang, Q.Z. Cheng, S.Q. Wang, Preparation and characterization of composite membranes of polysulfone and microcrystalline cellulose, *J. Appl. Polym. Sci.* 112 (2009) 550–556.
- [38] E. Celik, L. Liu, H. Choi, Protein fouling behavior of carbon nanotube/polyethersulfone composite membranes during water filtration, *Water Res.* 45 (2011) 5287–5294.
- [39] M.A.M. Motchelaho, H.F. Xiong, M. Moyo, L.L. Jewell, N.J. Coville, Effect of acid treatment on the surface of multiwalled carbon nanotubes prepared from Fe–Co supported on CaCO<sub>3</sub>: correlation with Fischer–Tropsch catalyst activity, *J. Mol. Catal. A Chem.* 335 (2011) 189–198.
- [40] L. Wang, L. Ge, T.E. Rufford, J.L. Chen, W. Zhou, Z.H. Zhu, V. Rudolph, A comparison study of catalytic oxidation and acid oxidation to prepare carbon nanotubes for filling with Ru nanoparticles, *Carbon* 49 (2011) 2022–2032.
- [41] S.T. Yang, J.X. Li, D.D. Shao, J. Hu, X.K. Wang, Adsorption of Ni(II) on oxidized multi-walled carbon nanotubes: effect of contact time, pH, foreign ions and PAA, *J. Hazard. Mater.* 166 (2009) 109–116.
- [42] S. Reza, M. Adeli, B. Astinchap, R. Kabiri, New nanocomposites containing metal nanoparticles, carbon nanotube and polymer, *J. Nanopart. Res.* 10 (2008) 1309–1318.
- [43] G.C.-R.A. Bottino, G. Capannelli, S. Munari, The formation of microporous polyvinylidene difluoride membranes by phase separation, *J. Membr. Sci.* 57 (1991) 1–20.
- [44] J.F. Blanco, J. Sublet, Q.T. Nguyen, P. Schatzel, Formation and morphology studies of different polysulfones-based membranes made by wet phase inversion process, *J. Membr. Sci.* 283 (2006) 27–37.
- [45] A. Rahimpour, M. Jahanshahi, S. Khalili, A. Mollahosseini, A. Zirepour, B. Rajaeian, Novel functionalized carbon nanotubes for improving the surface properties and performance of polyethersulfone (PES) membrane, *Desalination* 286 (2012) 99–107.
- [46] J.K. Shim, H.S. Na, Y.M. Lee, H. Huh, Y.C. Nho, Surface modification of polypropylene membranes by gamma-ray induced graft copolymerization and their solute permeation characteristics, *J. Membr. Sci.* 190 (2001) 215–226.
- [47] S. Qiu, L.G. Wu, X.J. Pan, L. Zhang, H.L. Chen, C.J. Gao, Preparation and properties of functionalized carbon nanotube/PSF blend ultrafiltration membranes, *J. Membr. Sci.* 342 (2009) 165–172.
- [48] P. van der Marel, A. Zwijnenburg, A. Kemperman, M. Wessling, H. Temmink, W. van der Meer, Influence of membrane properties on fouling in submerged membrane bioreactors, *J. Membr. Sci.* 348 (2010) 66–74.
- [49] J. Meng, L. Song, H.Y. Xu, H. Kong, C.Y. Wang, X.T. Guo, S. Xie, Effects of single-walled carbon nanotubes on the functions of plasma proteins and potentials in vascular prostheses, *Nanomedicine* 1 (2005) 136–142.
- [50] Z. Wang, H. Yu, J. Xia, F. Zhang, F. Li, Y. Xia, Y. Li, Novel GO-blended PVDF ultrafiltration membranes, *Desalination* 299 (2012) 50–54.